The 2009 IEEE/RSJ International Conference on
Intelligent Robots and Systems
October 11-15, 2009 St. Louis, USA

An Analysis Framework for Near Infrared Spectroscopy Based Brain-Computer Interface and Prospective Application to Robotic Surgery

Marco Caproni, Felipe Orihuela-Espina, David R. C. James, Arianna Menciassi, Paolo Dario, Ara W. Darzi and Guang-Zhong Yang

Abstract— **As medical robotics gathers increasing attention, the ergonomics of the surgical-console design becomes an important issue. Motivated by the need of augmenting the surgeon mastery, we explore the capabilities of a near infrared brain-computer interface as a complementary input modality to enhance the human-robot interaction at the robotic console. A multistage analysis framework is proposed and evaluated by an exploratory off-line synchronous study. The three stages of the data processing flow, namely dimensionality reduction, solution to binary problems and aggregation into multi-class decision are examined to address key challenges during the pattern recognition step. Early experimental results endorse near infrared based brain-computer interface as a suitable additional communication modality between the surgeon and the robotic console.**

I. INTRODUCTION

The application of robotic surgery is expanding due to its increased clinical uptake and clear advantages established in certain surgical specialties [1]. In particular, it is beneficial in minimally invasive surgery, where the technical demand on the surgeon is higher [2]. As robotic surgery becomes more common and the complexity of the attempted surgical procedures increases, the traditional input console is unable to provide the surgeon with ergonomically nature control of the action. For example, the surgeon has no haptic feedback and multitasking is difficult or even unviable. In general, the amount of manoeuvres required in surgical robotics increase with the complexity of the operation, and can lead to sensory overload. When under stress, this becomes a route cause of surgical errors. The potential solution to these problems can be addressed by the concept of *perceptual docking* [2], which represents a fundamental paradigm shift of perceptual learning and knowledge acquisition for robotic systems in that operator specific motor and perceptual/cognitive behaviour is acquired *in situ* through human-robot interaction. One recent work in the area is the use of gaze contingent control for improved visuo-motor coordination and attention selection [3]. However, it is unlikely that a single technology can provide a comprehensive solution to all the needs of human-robot interaction.

Marco Caproni is with Facoltà di Ingegneria, Università di Pisa, via Diotisalvi, 2, I-56126 Pisa, Italy. capronimarco@gmail.com

Arianna Menciassi and Paolo Dario are with Scuola Superiore Sant'Anna - CRIM Lab, P.za Martiri della Libertà, 33, I-56127 Pisa, Italy. arianna@sssup.it

Felipe Orihuela-Espina, David R. C. James, Ara W Darzi and Guang-Zhong Yang are with the Royal Wolfson Image Computing Laboratory and Department of Biosurgery and Surgical Technology, Imperial College London, United Kingdom. f.orihuela-espina@doc.ic.ac.uk

Near InfraRed Spectroscopy (NIRS) is a non-invasive, relatively affordable and portable neuroimaging modality that can detect cerebral blood flow as a surrogate for cortical activity. Unlike functional magnetic resonance , it allows the subject to have freedom of movement to perform a wide variety of tasks [4], [5]. The advent of wireless NIRS devices have further enhanced its use in normal control environments [6]. In complicated surgical tasks, NIRS can isolate discrete patterns of activation that can be related to the surgeon's intentions [4].

In brain-computer interface (BCI), the brain activity is reduced to an input command for controlling a cursor, a computer or a robotic device. BCI systems have now migrated from invasive (*e.g.* electrocorticography) to non invasive technologies, such as electroencephalography (EEG) and more recently NIRS. Although EEG remains the most popular since it retrieves the direct electrical activity of the brain, NIRS based BCI is gaining momentum [7], [8], [9]. NIRS has better spatial resolution compared to EEG, and therefore it is more consistent in extracting cortical responses for a given task. The existing work with NIRS based BCI make use of the indirect brain response based on neurovascular coupling. However, a fast direct response can also be recorded by NIRS [10], thus making it an attractive choice for BCI in the future, although specific hurdles remain to be addressed for the fast-NIRS signal [11].

Thus far, the predominant clinical application of BCI is in the control of prosthetic limbs [12]. In robotic surgery, BCI is an attractive candidate to reduce the above mentioned sensory overload and to enrich, as well as augment the surgeon-robot interface. This could be utilized to confirm the intention of an action, in the early detection of surgical errors and/or to assess psychological stress. In general, appropriateness of BCI in the field of surgical robotics remains largely unexplored.

The use of NIRS as an input for BCI is a relatively new topic in neuroimaging modality and consequently requires further work to assess its practical potential. In this context, there are pressing needs to develop a robust analysis framework for mapping NIRS response to intention and motor control. Motivated by this requirement, this study investigates the key data processing and pattern recognition challenges associated with the practical use of NIRS. The novelties

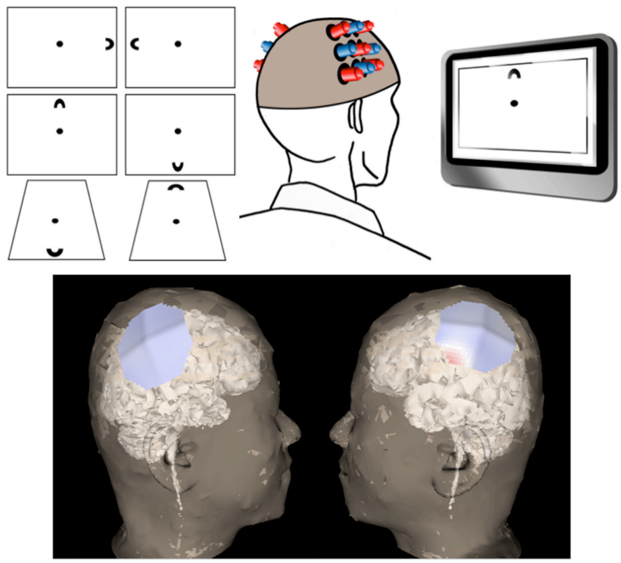

Fig. 1. Stimuli showing an object (circle) and a target (cup) in all possible 6 directions of 3D space (top left), a sketch of the experimental setup (top right) and the interrogated area over a brain atlas (bottom).

of the framework include a new feature selection strategy that takes into account meaningful sets of information, new conversion functions from binary to probabilistic outputs and a simple combination of classifiers strategy. We will use a simple motor control task to outline the key processing steps involved. We conclude by discussing potential applications in robotic surgery.

II. MATERIALS AND METHODS

An off-line synchronous BCI experiment in which 2 subjects mentally guiding an object towards a target in all 3D was designed. Using a block design paradigm, the subjects were exposed to 6 different stimuli in randomized sessions. Each session consisted of 30 second baseline rest period followed by three blocks of 20 seconds of stimulus and 30 seconds of rest. The stimulus consisted of a blank screen with an object and a target as illustrated in Fig. 1. The subject imagined moving the object into the target and instructions to do so were presented in two fashions; a) no specific instructions were given on how to move the target, non motor imagery (NMI), b) the subjects were instructed to imagine that they were pushing the object to the target using the right index finger, motor imagery (MI). The subjects completed 48 sessions (6 stimuli x 2 instruction modalities x 4 repetition) of 3 blocks each. Continuous wave NIRS measurement was obtained using a multi-channel HITACHI ETG-4000 optical topography system. Two arrays of 12 channels using a 3x3 optode configuration of light sources and detectors allow for a 24 channel recording. Interoptode distance was 3 cm. Channels were positioned according to the UI 10/10 system with the optode arrays centred at CP3 and CP4 [13].

Light measurements were converted to relative changes in oxy- and deoxyhaemoglobin using the modified Beer Lambert law [14]. The haemodynamic response was linearly detrended and decimated to 1 Hz. Task data was isolated and a 960D pattern vector was constructed using information from all 24 channels, 20 task-time samples and both haemoglobin species, $(24 \cdot 20 \cdot 2 = 960)$. Classification of the haemodynamic patterns was performed in a three stages analysis framework composed by a dimensionality reduction step, a binary pair-wise classification and a final aggregation unit of binary classifiers into a multi-class decision. This paper explores different possibilities for each of the stages.

A. Dimensionality reduction

The 960D space represents the haemodynamic brain response to moving the object towards the desired target. The *curse of dimensionality* [15] discourages the direct classification of patterns in this high dimensional space. In order to construct a valid reduced subset of features, two strategies were examined. In the first strategy, feature extraction was implemented using Isomap [16]. It has been previously demonstrated that Isomap is capable of capturing the haemodynamic brain response manifold [4]. The second strategy presents a feature selection process which emphasizes the importance of different time samples originating from a single chromophore signal at a particular location.

1) Feature Extraction: Isomap is a manifold embedding technique capable of unveiling the globally optimal solution [16]. Isomap can be summarized in two steps. First, an approximate estimation of the true geodesic distance along the manifold surface is computed. In our case, Floyd's algorithm has been applied using $r = 7$ nearest neighbours. Previous experience has taught us that the haemodynamic manifold is well captured with this value [4]. Second, classical multidimensional scaling (cMDS) is applied to the matrix of pair-wise distances to produce the output projection. The high dimensional 960D space was projected to either a 2 or 3 dimensional manifold. Adequacy of the projection is assessed by means of the distance distortion. Fixed Reference Isomap (FR-Isomap) [17] was designed to solve the problem of consistent embedding. In FR-Isomap, new points are projected on the reduced space generated by the references, in this case the training set. The projection coordinates of any new pattern are characterized from its nearest neighbours in the high dimensional space, by solving an optimization problem based on the Sammon's non-linear criterion [18].

2) Feature Selection - rSOMA-SFFS: A new feature selection algorithm has been developed to ensure that features are not treated blindly but in terms of significant blocks of information. Feature vectors were constructed by concatenation of all task samples of both haemoglobin species across all the recorded channels. As discussed, the 960D feature vector arises from η (number of task samples) samples per haemoglobin signal in the task period across all 24 channels. These features can be considered in meaningful subsets, or *SOMAs* (Subset Of Meaningful Attributes). A SOMA in this case refers to the subset of 20 features collected for a single chromophore at one single channel, for a total of 48 SOMAs. Each SOMA is then projected into a reduced SOMA (*rSOMA*) by the extraction of the first 2 principal components which contains more than 85% of the information in most SOMAs as illustrated in Fig. 2.

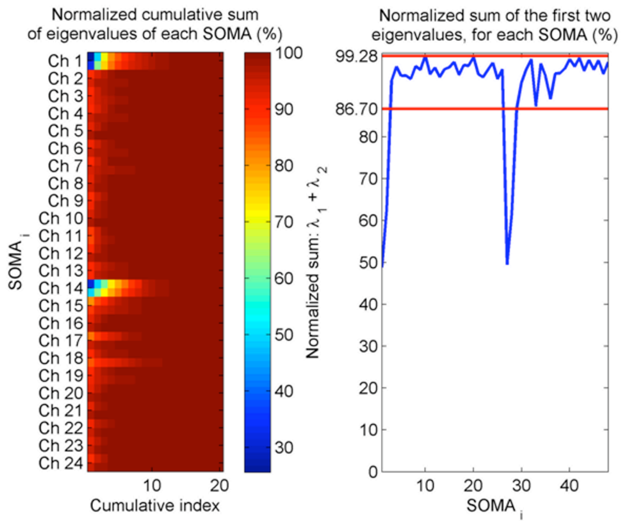

Fig. 2. PCA results on the SOMAs. The first two components account for more than 85% of the information in most cases.

A variation of the popular Sequential Floating Forward Selection (SFFS) [15], [19] has been implemented so that rSOMAs become indivisible groups of features that must be included or conditionally excluded as single entities to the current subset S_i. A block diagram of this algorithm is shown in Fig. 3. The classifier's classification error ϵ_c on the training set as the evaluation function was used . The three stopping criteria selected were reaching the maximum number of rSOMAs ($M = 8$), the maximum number of iterations ($I = 10^4$) or the 0% of classification error.

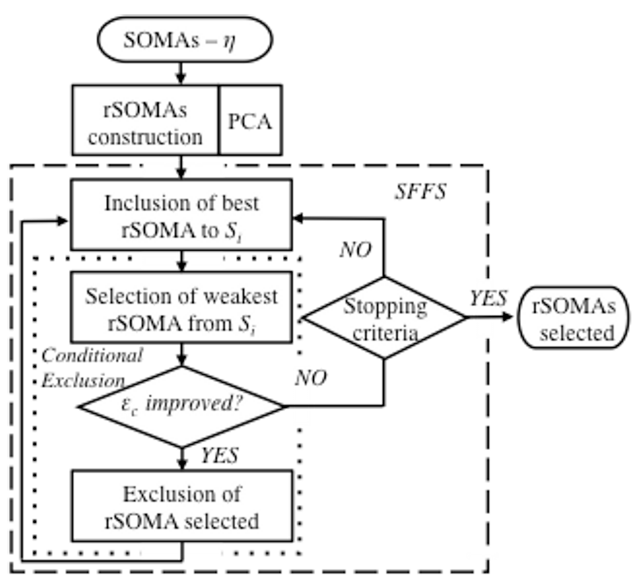

Fig. 3. rSOMA-SFFS algorithm block diagram. The algorithm groups features in meaningful subsets of information that can be added or discarded altogether.

B. Binary classifiers construction

After the dimensionality reduction stage, the multiclass problem was split into $K(K-1)/2 = 15$ binary decision sub-problems. Each binary classifier was learned using a Support Vector Machine (SVM). Since particular implementations of SVM may not lead to the optimum solution, each classifier were then allowed to be boosted using the AdaBoost algorithm. A *pick the best* strategy has been implemented to choose between SVM and AdaBoost classifier at every turn, the selection criterion being the smaller training error.

1) Support Vector Machines (SVM): Support Vector Machines are a family of classifiers which aim to find a hyperplane separating the classes so that the distance from the hyperplane to the patterns closest to it is maximal for optimum generalization capabilities [20], [21]. The payoff of the use of SVM over other classifiers is that they always find the global minimum. SVM has already been used for BCI with good results [8]. Perhaps, the more controversial issue when using SVM is the selection of the best kernel characterizing the classifier, which is still an open question [21]. In this study, a linear kernel was used. Slack variables ξ_i are introduced in the basic linear formulation in order to handle non-linearly separable problems:

$$\mathbf{x_i} \cdot \mathbf{w} + b \geq +1 - \xi_i \quad \text{for } y_i = +1 \tag{1}$$
$$\mathbf{x_i} \cdot \mathbf{w} + b \geq -1 + \xi_i \quad \text{for } y_i = -1 \tag{2}$$
$$\xi_i \geq 0 \quad \forall i. \tag{3}$$

In the above equation $\mathbf{x_i}$ are the patterns in the dataset and y_i are the class labels. The model parameters are the $< \mathbf{w}, b >$ which are established such that they optimize the cost function $L = \frac{\|\mathbf{w}\|^2}{2} + C\left(\sum_i \xi_i\right)^k$, where C is the regularization constant introduced to penalize misclassifications. A value $k = 1$ was selected. Moreover, a value of 10^{-3} for the regularization constant was selected since we found this value to be in the range that avoids extreme behaviours, overfitting and random results. The optimization problem is solved using a constrained formulation of Lagrangian multipliers. The STPR toolbox [22] was used to implement SVM classifiers.

2) AdaBoost: Practical limitations of SVM implementations may lead to a suboptimal selection of the class separating hyperplane [23]. Originally developed for improving the performance of weak classifiers such as PAC, AdaBoost can enhance the performance of a weak learner closer to the Bayesian limit [24]. Each binary classifier $h_t(\mathbf{x})$ was given the chance to improve using the AdaBoost algorithm, before proceeding to aggregation on a multi-class classifier. The boosting is achieved by modifying the distribution of weights over the patterns in the training set: on each iteration, the distribution is re-weighted so that patterns which are more difficult to classify are given more weight than those easier to classify. In this way, AdaBoost emphasises on those regions harder to separate and a non-linear classifier $H(\mathbf{x})$ is built upon the decision made by multiple simple linear classifiers (5):

$$f(\mathbf{x}) = \sum_{t=1}^{T} \alpha_t h_t(\mathbf{x}) \quad (4)$$

$$H(\mathbf{x}) = sign(f(\mathbf{x})) \quad (5)$$

where α_t are the coefficients assigned to each classifier $h_t(\cdot)$, based on its training error ϵ_t according to (6):

$$\alpha_t = \frac{1}{2} log \left(\frac{1-\epsilon_t}{\epsilon_t} \right) \quad (6)$$

AdaBoost was run using a maximum of $T = 20$ classifiers.

C. Aggregation of binary classifiers

Finally, aggregation of the 15 binary classifiers into a single multiclass classifier was attempted using three voting strategies:

1) Majority Voting (MV): each binary classifier cast a vote. Current pattern is assigned to the class with more votes. In case of draw, the current pattern is assigned to the null class 0, that means that no decision can be done. Random selection has been suggested as a solution under draws, but a 0-class strategy is more conservative.

2) Weighted Majority Voting (WMV): again, each binary classifier casts a vote y_k. As opposed to the previous scheme, votes have different weights μ_k, according to the margin of the binary classifier that produced them. Patterns x are assigned to the class ω_i that has the maximum score after the weighted voting stage. In case of draw, the classifier with the smallest margin is discarded and the weighted votes are counted again.

3) Correcting Classifiers (CC): correcting classifiers aim to tackle the nonsense introduced by considering a binary classifier's output when the pattern under consideration belongs to neither of the two classes it was trained with [25]. The output of the binary classifier that separates class ω_i from ω_j is interpreted as a probability of membership to ω_i, $\hat{p}_{ij}$. To convert the binary output of a SVM in such a measure, the function (7) and shown in Fig. 4 is proposed.

$$\hat{p}_{ij} = \frac{1}{1 + e^{\frac{-d}{m}}} \quad (7)$$

where d is the distance of the pattern from the separating hyperplane in SVM, or the final score $f(\mathbf{x})$ in AdaBoost, and m is the margin. Another possible function is the one proposed in [27]. Each i-*vs*-j classifier is then complemented with a correcting classifier (i, j)-*vs-all* yielding an output $\hat{q}_{ij}$ capturing the probability of new patterns belonging to $\omega_i \bigcup \omega_j$. These values are then used to calculate the probability of each class $\hat{p}_i$ (8):

$$\hat{p}_i = \frac{2}{K(K-1)} \sum_{j \neq i} \hat{p}_{ij} \cdot \hat{q}_{ij} \quad (8)$$

Finally, the aggregation policy is given by (9).

$$arg \max_{1 \leq i \leq K} \hat{p}_i \quad (9)$$

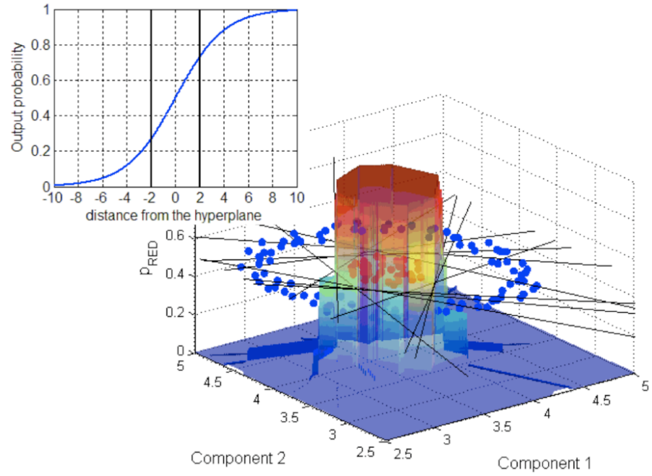

Fig. 4. Conversion from binary output to probabilistic output for SVM (top left) and AdaBoost (bottom right).

III. RESULTS AND DISCUSSION

For each of the two instruction paradigms - motor imagery (MI) and non motor-imagery (NMI) - a number of simulations were carried out using the proposed scheme. The number of simulation was the result of using 3 different channel selections (left only, right only and all channels), two underlying classifiers (SVM and AdaBoost), three aggregation policies (MV, WMV and CC), and a varying number of binary classifiers depending on the directions being classified. To make the most of the small test set, the simulations were made with the split between training set and test set at either 75%-25% or 80%-20% respectively. Ten runs were made for each valid combination, with the dataset being pick at random from the pool.

A. Instruction paradigm and multichannel information

The results of the simulations were split into six groups as result of two instruction paradigms and three possible attendance to channels; right only channels (channels 1 to 12), left only channels (channels 13 to 24), or all channels together. A non-parametric multigroup Kruskal-Wallis test indicated that not all tested configurations present the same median. The multiple comparison procedure based on *t*–test with 95% confidence level and a Bonferroni correction proved that there is a statistically significant difference between the two instruction paradigms. It is the NMI which show a better performance. This is in agreement with Luu and Chau [9] suggestion than non forcing a common strategy may be a more intuitive for BCI systems as this requires less cognitive load. In terms of the channels, the use of right only channels under NMI has a statistically significantly better performance than using the channels on the right. This suggests that it may be easier to separate the ipsilateral motor response despite being smaller in intensity. However the channels in the contralateral side may still give a small contribution as using

TABLE I

CLASSIFICATION ACCURACY FOR EACH PARTICIPANT ALONG THE MAIN DIRECTIONS

Direction	Subject 1		Subject 2	
	Input	$\mu \pm \sigma$	Input	$\mu \pm \sigma$
U/D	MI/Left FE (2D)	0.67 ± 0.20	MI/Left FE (3D)	0.55 ± 0.17
L/R	MI/Left FE (3D)	0.57 ± 0.25	MI/Left FE (2D)	0.61 ± 0.18
B/F	NMI/Right FE (2D)	0.62 ± 0.22	NMI/Left FE (3D)	0.65 ± 0.22

all channels slightly outperforms using only the ipsilateral information, but this did not reach statistical significance.

B. Separation of single directions

Tab. I reports the classification accuracy for each participant, for its optimal combination of instruction paradigm, multi-channel information and dimensionality reduction technique, with the 75%-25% partition. In this particular exercise, the Feature Selection algorithm did not outperform Feature Extraction. However, the difference did not reach statistical significance. Whilst Feature Extraction yields the top performance in cases where half of channels are taken into account, Feature Selection marginally performs better if all channels are considered. This hints that the proposed rSOMA-SFFS algorithm is able to learn automatically the optimal subset of information needed. The *pick the best* strategy consistently behave as a compromise between both classifiers as illustrated in Fig. 5.

Depth perception in 2D displays benefits from cues that include perspective, occlusion, size and shadows [26]. The wireframed stimulus here used includes standard one-pointperspective, but none of the other cues. As emanates from Fig. 5, the perspective cue is sufficient to facilitate the control along the third dimension (B/F) for which the classification rates are in range with rates along the other two remaining dimensions.

C. Separation of multiple directions

The non normal but symmetric behaviour of the three groups of simulation corresponding to the three aggregation policies - MV, WMV and CC - was assessed by means of QQ plots, histograms and boxplots (not shown). A Kruskal Wallis test was applied and found statistical significance that at least one of the group has a different median.

A subsequent multiple comparison test shows that majority voting aggregation policy producing the weakest results reached statistical significance. In between weighted majority voting and correcting classifiers, it is the latter who yields better results, however this is inconclusive, as statistical significance was not reach as illustrated in Fig. 6. The combination of potentially conflicting decisions by multiple classifiers remains an unsolved problem [28].

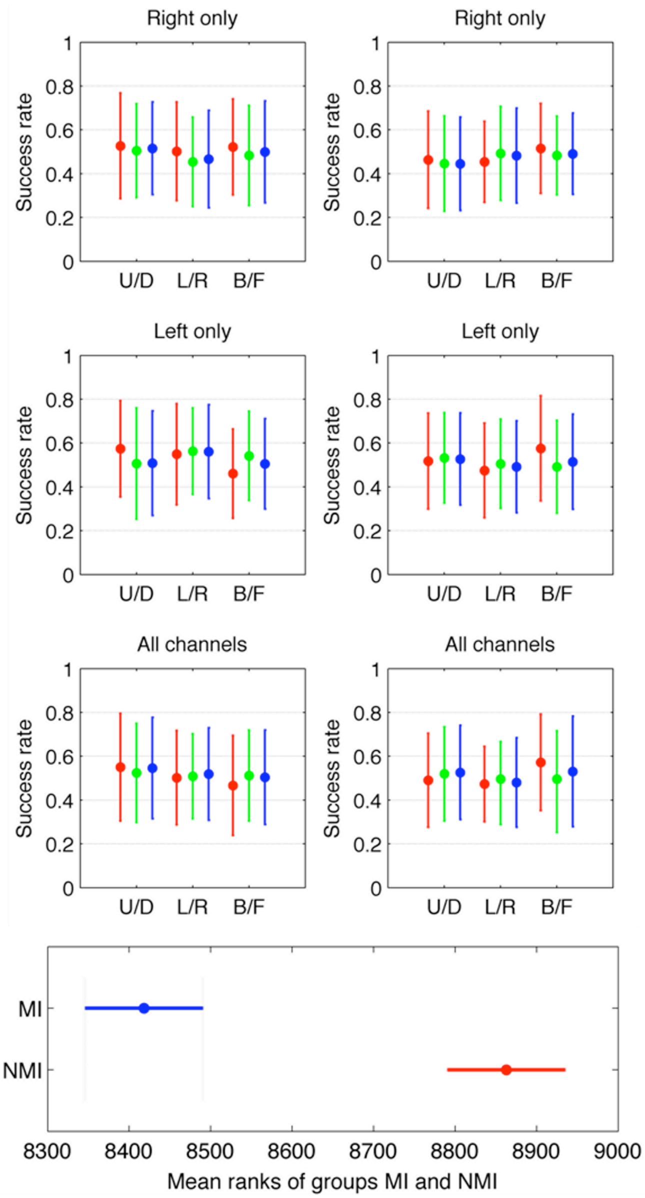

Fig. 5. The first six panels show the classification success rate (average of both subjects) by SVM (red), AdaBoost (green) and pick the best strategy (blue). Left column plots correspond to MI, and right column to NMI. The panel below shows a mean ranks t-test with 95% confidence level and a Bonferroni correction for MI and NMI groups.

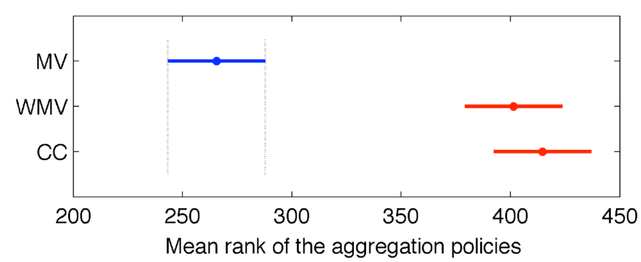

Fig. 6. Mean ranks t-test with 95% confidence level and a Bonferroni correction.

IV. CONCLUSIONS AND FUTURE WORK

In this paper we have developed a comprehensive haemodynamic pattern classification framework for its potential use in robotic control. The analysis framework was evaluated under the perspective of a visuo-motor stimulus. Being an initial explorative study, the sample size used in study is admittedly small and the small training size may have hindered higher classification rates. The total training time is in line with similar published works [7], [8] . Nevertheless, the study has outlined practical potential of this promising approach. In the light of these results, we suggest that a NIRS based BCI has potential to complement existing human-machine interfaces. Prospective early applications may be, for example, corroboratory selector switch of surgical decision, selection of robot movement alternative pre-loaded paths with adaptive active constraints and/or early identification of mental weariness. It is expected that application to surgical robot arm direct movement control requires further ethical and safety considerations.

V. ACKNOWLEDGMENTS

We gratefully acknowledge the contribution of the European Community's 7th Framework Programme for the funding received for the ARAKNES project ((IP)-ICT-2007-2#224565).

REFERENCES

[1] J. Marescaux and F. Rubino, "Robotic surgery: potentials, barriers and limitations", *European Surgery-Acta Chirurgica Austriaca*, vol. 37(5), 2005, pp. 279-283.

[2] G. Z. Yang, G. P. Mylonas, K.-W. Kwok, and A. Chung, "Perceptual Docking for Robotic Control", *In Proceedings of the Fourth Medical Imaging and Augmented Reality, MIAR*, Tokyo, Japan, Lecture Notes in Computer Science, vol. 5128, 2008, pp. 21-30.

[3] G. P. Mylonas, K-W. Kwok, A. W. Darzi, and G. Z. Yang, "Gaze-Contingent Motor Channelling and Haptic Constraints for Minimally Invasive Robotic Surgery", *In Proceedings of the Medical Image Computing and Computer-Assisted Intervention (MICCAI'08)*, New York, USA, Lecture Notes in Computer Science, vol. 5242, 2007, pp. 676-683.

[4] D. R. Leff, F. Orihuela-Espina, L. Atallah, A. W. Darzi and G. Z. Yang, "Functional Near Infrared Spectroscopy in Novice and Expert Surgeons: a Manifold Embedding Approach", *In Proceedings of the Medical Image Computing and Computer-Assisted Intervention (MICCAI '07)*, Brisbane, Australia, Lecture Notes in Computer Science, vol. 4792, 2007, pp. 270-277.

[5] D. R. Leff, C. E. Elwell, F. Orihuela-Espina, L. Atallah, D. T. Delpy, A. W. Darzi and G. Z.Yang, "Changes in prefrontal cortical behaviour depend upon familiarity on a bimanual co-ordination task: An fNIRS study", *NeuroImage*, vol. 39, 2008, 805-813.

[6] Y. Hoshi, "Functional Near-Infrared Spectroscopy: Current Status and Future Prospects", *Journal of Biomedical Optics*, vol. 12(6), 2007, pp. 062106.

[7] S. M. Coyle, "Brain-Computer Interface Using a Simplified Functional Near-Infrared Spectroscopy System", *Journal of Neural Engineering*, vol. 4, 2007, pp. 219-226.

[8] R. Sitaram, H. Zhang, C. Guan, M. Thulasidas, Y. Hoshi, A. Ishikawa, K. Shimizu and N. Birbaumer, "Temporal Classification of Multichannel Near-Infrared Spectroscopy Signals of Motor Imagery for Developing a Brain-Computer Interface", *NeuroImage*, vol. 34, 2007, pp. 1416-1427.

[9] S. Luu and T. Chau, "Decoding subjective preference from single trial near-infrared spectroscopy signals", *Journal of Neural Engineering*, vol. 6, 2009, pp. 016003.

[10] M. A. Franceschini and D. A. Boas, "Noninvasive Measurement of Neuronal Activity with Near-Infrared Optical Imaging", *NeuroImage*, vol. 21, 2004, pp. 372-386.

[11] H. Radhakrishnan, W. Vanduffel, H.P. Deng, L. Ekstrom, D. A. Boas and M. A. Franceschini, "Fast Optical Signal Not Detected in Awake Behaving Monkeys", *NeuroImage*, vol. 45, 2009, pp. 410-419.

[12] S. G. Mason, A. Bashashati, M. Fatourechi, K. F. Navarro, and G. E. Birch, "A Comprehensive Survey of Brain Interface Technology Designs", *Annals of Biomedical Engineering*, vol. 35(2), 2007, pp. 137-169.

[13] V. Jurcak, D. Tsuzuki, and I. Dan, "10/20, 10/10 and 10/5 System Revisited: Their Validity as a Relative Head-Surface-Based Positioning Systems", *NeuroImage*, vol. 34, 2007, pp. 1600-1611.

[14] D. T. Delpy, M. Cope, P. van der Zee, S. R. Arridge, S. Wray and J. S. Wyatt, "Estimation of Optical Pathlength Through Tissue from Direct Time of Flight Measurement", *Physics in Medicine and Biology*, vol. 33(12), 2007, pp 1433-1442.

[15] A. K. Jain and D. Zongker, "Feature Selection: Evaluation, Application, and Small Sample Performance", *IEEE Transactions on Pattern Analysis and Machine Intelligence*, vol. 19, 1997, pp. 153-158.

[16] J. B. Tenenbaum, V. de Silva and J. C. Langford, "A Global Geometric Framework for Nonlinear Dimensionality Reduction", *Science*, vol. 290, 2000, pp. 2319-2323.

[17] K. Lekadir, D. S. Elson, J. Requejo-Isidro, C. Dunsby, J. McGinty, N. Galletly, G. Stamp, P. M. W. French, and G. Z. Yang, "Tissue Characterization Using Dimensionality Reduction and Fluorescence Imaging", *In Proceedings of the Ninth Medical Image Computing and Computer-Assisted Intervention (MICCAI '06)*, Copenhagen, Denmark, Lecture Notes in Computer Science, vol. 4191, 2006, pp. 586-593.

[18] J. W. Sammon, "A Nonlinear Mapping Algorithm for Data Structure Analysis", *IEEE Transactions Computers*, vol. 18, 1969, pp. 401-409.

[19] P. Pudil, F. J. Ferri, J. Novovičová and J. Kittler, "Floating Search Methods for Feature Selection with Non-Monotonic Criterion Functions", *In Proceedings of the Twelveth International Conference on Pattern Recognition, IAPR*, Jerusalem, Israel, 1994, pp. 279-283.

[20] E. Alpaydin, *Introduction to Machine Learning*, MIT Press, Cambridge, Mass, 2004.

[21] C. J. C. Burges, "A Tutorial on Support Vector Machines for Pattern Recognition", *Data Mining and Knowledge Discovery*, vol. 2, 1998, pp. 121-167.

[22] V. Franc, V. Hlavàč, "Statistical Pattern Recognition Toolbox for Matlab", Technical report, Czech Technical University, 2004.

[23] H. C. Kim, S. Pang, H.-M. Je, D. Kim , S. Y. Bang, "Constructing support vector machine ensemble", *Pattern Recognition*, vol. 36, 2003, pp. 2757-2767.

[24] Y. Freund and R. E. Schapire, "A Decision-Theoretic Generalization of On-Line Learning and an Application to Boosting", *Journal of Computer and System Sciences*, vol. 55, 1997, pp. 119-139.

[25] M. Moreira and E. Mayoraz, "Improved Pairwise Coupling Classifiers with Correcting Classifiers", *Proceedings of Tenth European Conference on Machine Learning*, Chemnitz, Germany, Lecture Notes in Computer Science, vol. 1398, 1998, pp. 160-171.

[26] L. Kjelldahl, "A study on how depth perception is affected by different presentation methods of 3D objects on a 2D display", *Comput. & Graphics*, vol. 19(2), 1995, pp. 199-202.

[27] J. C. Platt, "Probabilistic Outputs for Support Vector Machines and Comparisons to Regularized Likelihood Methods", *Advances in Large Margin Classifiers*, MIT Press, 1999

[28] T. K. Ho, J. J. Hull, S. N. Srihari, "Decision Combination in Multiple Classifier System", *IEEE Transaction on Pattern Analysis and Machine Intelligence*, vol. 16(1), 1994, pp. 66-75.